Supporting Information

How to Unravel the Chemical Structure and Component Localization of Individual Drug-Loaded Polymeric Nanoparticles by Using Tapping AFM-IR

Jérémie Mathurin[#a] Elisabetta Pancani[#b], Ariane Deniset-Besseau[a], Kevin Kjoller[c], Craig B. Prater *[c], Ruxandra Gref*[b], Alexandre Dazzi* [a].

Table S1 - Hydrodynamic diameter of unloaded and loaded NPs. NP mean diameter was determined by both DLS and NTA. For DLS measurements data are reported as Z average and as number distribution to allow the comparison with NTA results.

Formulation	Mean diameter			
	DLS Z average (nm ± SE)	**PdI**	**DLS** Number average (nm ± SD)	**NTA** (nm ± SD)
Unloaded PLA NPs	255 ± 4	0.059	228 ± 66	170 ± 45
Unloaded PLGA NPs	244 ± 2	0.064	208 ± 60	140 ± 40
PIP-loaded PLGA NPs (nanoemulsion)	229 ± 3	0.067	189 ± 58	150 ± 40
PIP-loaded PLGA NPs (precipitation)	161 ± 2	0.079	117 ± 34	126 ± 26

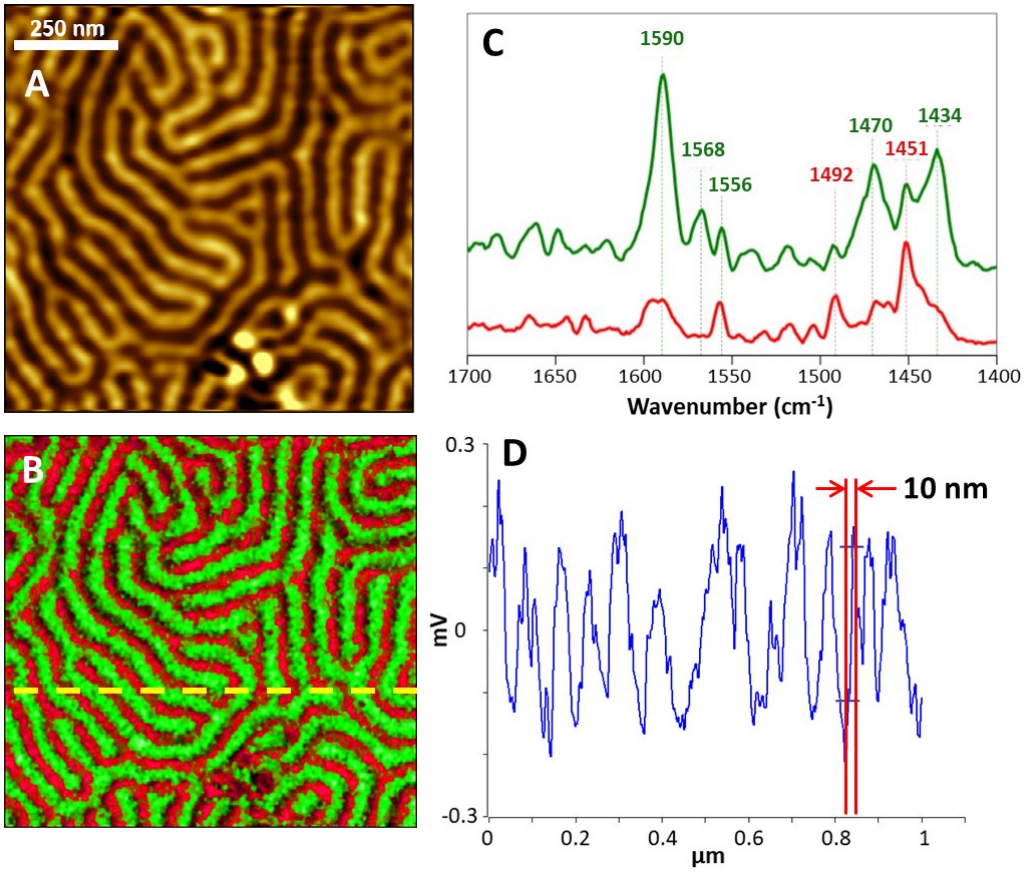

Figure S1 – Tapping AFM-IR images and spectra of a PS-P2VP Block Copolymer sample demonstrating the high spatial resolution of the technique. The PS-P2VP sample was imaged with a scan size of 1 x 1 µm, the height image (A) clearly shows the two components that compose the sample. Tapping AFM-IR images were collected at two absorption bands specific to PS (1492 cm-1, red) and P2VP (1588 cm-1, green) and the images were aligned and overlapped (B) allowing clear chemical identification of the two components. This identification is confirmed in the Tapping AFM-IR spectra (C) collected from the two materials. Shown in (D) is a cross section of one of the chemical images demonstrating a spatial resolution of <10 nm. For the resolution estimation here, the authors have taken the smallest feature of the chemical image and measure the distance over which the signal changes from 90% to 10%. This sample was provided courtesy of the University of Bordeaux, Dr. Pecastaings.

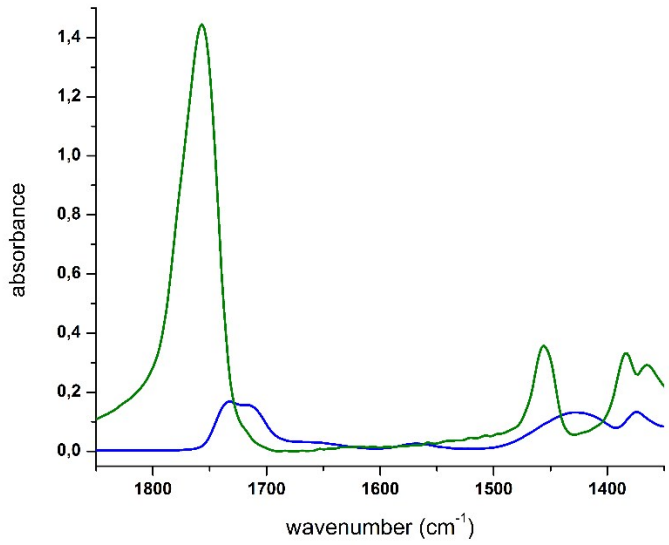

Figure S2 – IR spectra of bulk PLA and PVA in the range 2000-1350 cm^{-1}. In green: spectrum of PLA characterized by the ester carbonyl band at 1756 cm^{-1} and by the C-H bending of CH_2 and CH_3 at 1455, 1382 and 1365 cm^{-1}. In blue: spectrum of PVA showing the carbonyl band of the un-hydrolyzed acetate at 1710 cm^{-1} and the C-H bending in the 1500-1350 cm^{-1} range (1420 and 1370 cm^{-1}).

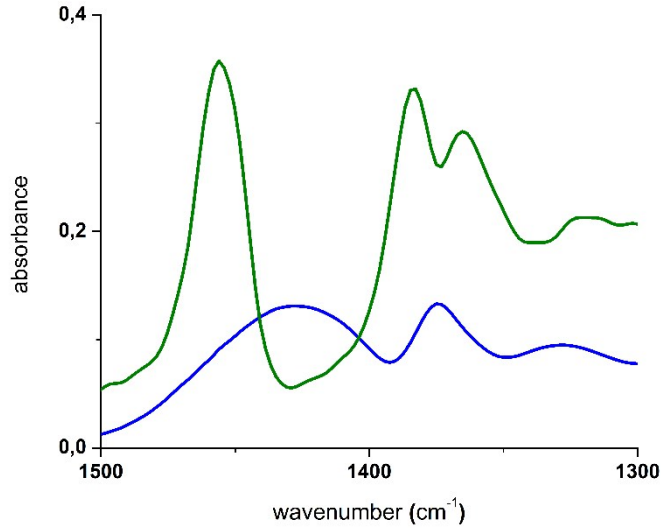

Figure S3 – IR spectra of bulk PLA and PVA in the range 1500-1300 cm^{-1}. In green: spectrum of PLA characterized by C-H bending of CH_2 and CH_3. In blue: spectrum of PVA showing its C-H bending bands which have different positions compared to the PLA. Indeed, the PVA band at 1420 cm^{-1} stand out from the PLA spectrum and could thus be used as a fingerprint to undoubtedly detect PVA localization.

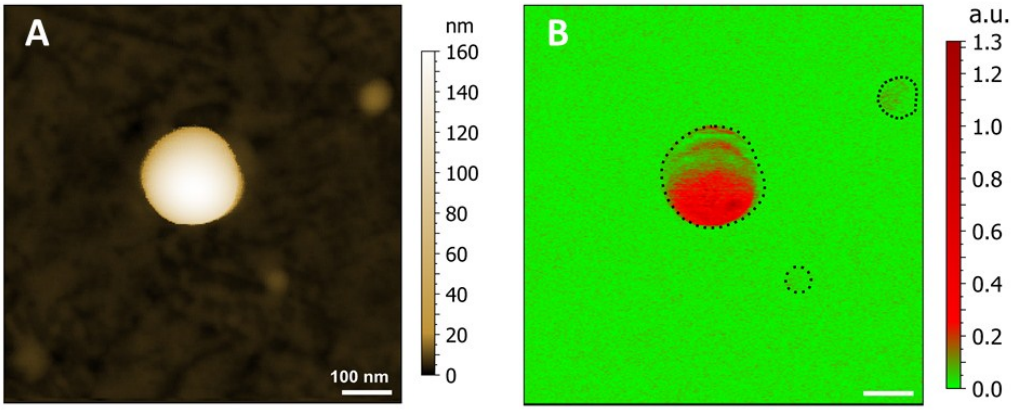

Figure S4 - AFM-IR study of empty PLGA NPs (complementary to Figure 4, Main text). A) Topography image of the PLGA NPs. B) Tapping AFM-IR map at 1760 cm^{-1} corresponding to a very strong absorption of the carbonyl ester group (C=O stretching) of PLGA.

Phase shift

In **Figure 4** of the main text (and in **Figure S4** and **S6**) some NPs displayed a lack of intensity with a moon crescent shape in the chemical maps (**Figure 4B** and **4D**) which was attributed to phase shifts. Indeed, the IR signal at the upper part of the big NP in the center of the region of interest (ROI) is not complete and does not match well with the NP topography. The phase image (**Figure 4C, Main text**) corresponding to these maps can clearly explain this effect. Given the size of this NP (around 160 nm), the tip contact changes considerably during the IR mapping acquisition thus leading to an excessive and sudden phase change. As a consequence, the resonance of the 1st mode does not match the laser repetition rate, making the 2nd excitation mode decrease. In our experimental settings, the AFM set point of the driving tapping mode (1st) was regulated to produce a soft contact (80% of free amplitude) thus avoiding an excessive pressure on the NPs.

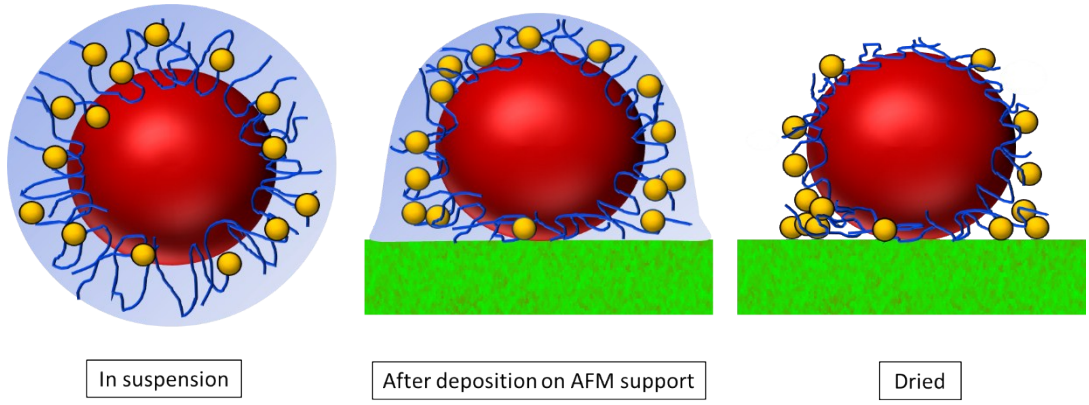

Figure S5 - Schematic representation of the deposition and drying process of a PIP-loaded PLGA NP on an AFM support. During the drying process, PVA chains are progressively dehydrated and thus flattened on the NP surface or deployed on the AFM support. The thickness of the corona is therefore reduced and deformed during the drying phase. The PIP, which has an affinity for PVA, follows the PVA chains movement and is preferentially deposited at the NP border in the interstices with the support.

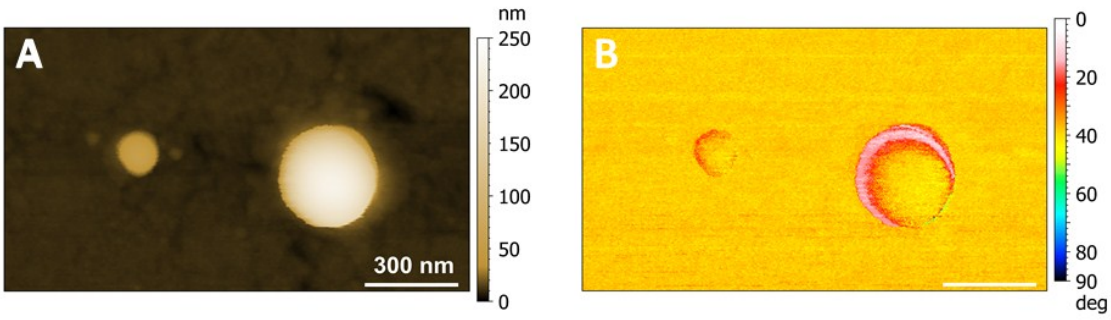

Figure S6 - AFM-IR study of PIP-loaded PLGA NPs prepared by nanoemulsion (complementary to Figure 5, Main text). A) Topography of PIP-loaded nanoemulsion PLGA NPs. B) Phase image associated to the topography showing the croissant moon shape effect which explains the lack of intensity in the IR image.